RSC Advances

ROYAL SOCIETY OF CHEMISTRY

www.rsc.org/advances

Journal Name

RSCPublishing

ARTICLE

Locked Nucleic Acid modified bi-specific aptamer-targeted nanoparticles carrying survivin antagonist towards effective colon cancer therapy

Cite this: DOI: 10.1039/xoxxooooox

Received ooth January 2012,
Accepted ooth January 2012

DOI: 10.1039/xoxxooooox

www.rsc.org/

Kislay Roy[1], Rupinder K. Kanwar[1], Chun Hei Antonio Cheung[2,3], Cassandra Lee Fleming[4], Rakesh N. Veedu[5], Subramanian Krishnakumar[6] and Jagat R. Kanwar[1]*

We investigated the anti-cancer activity of alginate coated chitosan nanoparticles (CHNP) encapsulating cell-permeable dominant negative survivin (SR9) with locked nucleic acid (LNA) aptamers targeting EpCAM and nucleolin (termed as "nanobullets") in in vitro (2D and 3D cell culture models) and in vivo (colon cancer mouse xenograft model). We incorporated three LNA modifications in each sequence in order to enhance the stability of these aptamers. Confocal microscopy revealed binding of the LNA-aptamers to their specific markers with high affinity. The muco-adhesive nanobullets showed 6-fold higher internalization in cancer cells when compared to non-cancerous cells, suggesting a tumour specific uptake. A higher intensity of nanobullets was observed in both periphery and core of the multicellular tumour spheroids compared to non-targeted CHNP-SR9. The nanobullets were found to be the highly effective as they led to a 2.26 fold ($p < 0.05$) reduction at 24 h and a 4.95 fold reduction ($p \leq 0.001$) fold reduction in the spheroid size at 72 h. The tumour regression was 4 fold higher in mice fed on nanobullet diet when compared to control diet. The nanobullets were able to show a significantly high apoptotic ($p \leq 0.0005$) and necrotic index in the tumour cell population ($p \leq 0.005$) when compared to void NPs. Therefore, our nanoparticles have shown highly promising results and therefore deliver a new conduit towards the approach of cancer-targeted nanodelivery.

INTRODUCTION

Colorectal cancer (CRC) is the third-leading cause of cancer-related deaths in developed countries, and its incidence is steadily rising in developing countries [1]. Unfortunately, the conventional adjuvant treatments have shown only modest effects on long-term survival after surgical resection [2, 3]. Therefore, an urgent need for novel therapies to treat colon cancer is required. It has been reported that majority of the CRCs show APC mutation, which in turn is directly linked with overexpression of survivin, as the wt-APC protein coded by the APC gene is known to suppress the survivin expression[4]. Using polymerase chain reaction (PCR), a dominant negative survivin (SR9) (replacing cysteine by alanine at 84th position, SurC84A) protein was fused with the cell penetrating peptide poly-arginine (9 residues of arginine, R9) and was expressed in *E. coli* using PGE2TX vector and purified by affinity chromatography. We demonstrated in our previous studies that SR9 successfully penetrated into 3D-cultured HeLa and DU145 cells and induced cancer cell death. It was observed that caspase-9 and caspase-3 were upregulated[5].

Epithelial cell adhesion molecule (EpCAM) is a type I membrane protein expressed in a variety of human epithelial tissues and cancer. In normal cells EpCAM is predominantly located in intercellular spaces or in the cytoplasm. Therefore, it is speculated that EpCAM in normal cells is much less accessible to antibodies than EpCAM in cancer tissues [6]. It is known that EpCAM expression is not limited to CSCs, and EpCAM expression has been frequently shown in breast, colon, pancreas and prostate cancers however, CSCs overexpress EpCAM when compared to cancer cells [7]. In a study to determine the role of EpCAM in CRC CSCs, solid CRC tissues were disaggregated into-single cell suspension and sorted on the basis of surface markers, these sorted cells were further injected into NOD/SCID mice to investigate their tumorigenic potential. It was observed that EpCAM/CD44 positive cells maintained high tumorigenicity and therefore, proving that EpCAM is a CSC marker in CRC [8].

Nucleolin is a RNA binding protein (RBP) which is prominently abundant in nucleolus and interacts with RNA-recognition motifs (RNMs) and helps in cell proliferation [9]. Nucleolin is also known to be expressed on the cell surface in many cancer cells and therefore, has been recognized as a cancer marker [10, 11]. It has been proved that although nucleolin is a nucleolar protein it can translocate to the cell surface via small vesicles [12]. Functional form of nucleolin molecule has been majorly found in actively dividing cells whereas, only the degraded form of nucleolin has been found in non-dividing cells suggesting that the nucleolin molecule is cell proliferation dependent [13]. It has also been shown that normal cells have lower levels of nucleolin in both plasma membrane and cytoplasm [14].

Therefore, we chose to target both EpCAM and nucleolin as they are established cell surface receptor proteins [15, 16] that are highly over-expressed in most cancer cells [17, 18] and are known to translocate into the nucleus as a full length molecule and in their splice forms[19, 20] which may facilitate enhanced uptake of the therapeutic (Figure 1). Nucleic acid aptamers are short single-stranded (ss) DNA or RNA sequences which fold into 3D structures that bind to their target sites with high specificity and affinity and have often been used to selectively target various forms of tumour [21, 22]. Due to its unprecedented target binding affinity and excellent nuclease resistance locked nucleic acid (LNA) is one of the most prominent and successful modified nucleotides developed in recent years [23].

Recently, we found that a cell-permeable dominant negative survivin (SurR9-C84A, referred to as SR9) competitively inhibited

endogenous survivin and blocked the cell cycle at the G_1/S phase. The nanoencapsulation of SR9 in chitosan nanoparticles (CHNP-SR9) increased its stability, protected primary cells from autophagy and successfully induced tumor-specific apoptosis via both extrinsic and intrinsic apoptotic pathways. However, lack of cancer specific targeting led to high accumulation of these nanoparticles in bone, blood, kidney, brain and intestines [24]. Cancer specific targeting of CHNP may ensure a higher delivery of SR9 to the tumour site an increase in their anti-cancer efficacy. Hence, in the present study, we have decorated alginate coated CHNP-SR9 with LNA aptamers targeting EpCAM and nucleolin (termed as "nanobullets"). The biophysical characterisation for both LNA modified aptamers has been reported here for the first time along with an in vitro (2D and 3D cell culture models) and in vivo (colon cancer mouse xenograft model) analysis to determine the anti-cancer activity of these nanobullets.

MATERIAL AND METHODS

Materials

Mouse anti-EpCAM, anti-nucleolin antibody and mouse monoclonal anti-survivin antibody were purchased from Santa Cruz Biotechnology (Santa Cruz, CA). Anti-mouse FITC, anti-rabbit FITC/TRITC, anti-goat FITC/TRITC, and anti-mouse horse-raddish per-oxidase (HRP) antibodies were purchased from Sigma Aldrich (St. Louis, MO). The EpCAM LNA modified aptamer (LNA-Ep, 5'-**G**CGACUG**G**UUACCCGGUC**G**-3'), scrambled (5'-**G**CGACUG**G**UAUCGGGGUC**G**-3') and the nucleolin LNA modified aptamer (LNA-Nu, 5'-**G**GTGGTGGTG**G**TTGTGGTGGTGGTG**G**-3'), scrambled (5'-**G**GTGGTGGTG**G**GGTGGTTGGTGGTG**G**-3') were both synthesized by RiboTask, (Denamrk). Chemicals such as low molecular weight chitosan, sodium tri-poly phosphate (STPP), alginate, rhodamine, and 5-fluorouracil (FU) were all purchased from Sigma Aldrich (St. Louis, MO). Annexin V staining kit was purchased from Invitrogen (NSW, Australia).

Biophysical characterisation of LNA aptamers

CD spectra of samples were recorded on a JASCO J-815 CD spectrophotometer purchased from ATA scientific (NSW, Australia) under nitrogen atmosphere at room temperature. Data was collected from 220 nm to 340 nm using a quartz cuvette of 1 mm pathlength. The datapitch was set to 0.1 nm, scanning rate to 50 nm/min and bandwidth to 1 nm. On an average of 4 accumulations per scan was obtained. In order to characterise the LNA aptamers using nuclear magnetic resonance (NMR), the samples were dissolved in 10% D_2O/H_2O and the 1D ^1H NMR spectrum of the samples were obtained at 500 MHz using a Bruker Advance 500SB spectrometer.

Serum stability of LNA aptamers

The serum stability of the aptamers were tested after diluting the aptamers in 1:50 dilution PBS with 10% serum and incubated for 0h to 96h. The dilutions were then run on polyacrylamide gel electrophoresis (PAGE) at 100V for 35 min and visualized using the Chemi-doc with XRS camera.

Cell culture

The colon cancer cells (Caco-2 and SW480) and healthy human intestinal cells (FHs 74 Int) were obtained from the American type culture collection (ATCC) and were grown in tissue culture flasks using Dulbecco's minimum essential medium (DMEM) containing high glucose, L-glutamine and sodium pyruvate (GIBCO), supplemented with 20% heat inactivated foetal bovine serum (FBS) (Sigma Aldrich, Australia). Penicillin/streptomycin was added in a concentration of 0.1 mg/ml to prevent growth of unwanted

microorganisms and the culture was maintained at 37°C in 5% CO_2 to maintain a saturated humid atmosphere. After every 2-3 days of culturing, the media in the flask was replaced with fresh media.

Immunofluorescence studies using confocal microscopy

Cells were seeded in 8 chambered slides and treated with the respective treatments. Post treatment interval, media was removed from the chambers and cells were fixed using 4% paraformaldehyde (PF) for 20 min at 37°C. Cells were permeabilized using 0.01% triton-X100 for 5 min. Cells were further blocked with 3% bovine serum albumin (BSA) for 30 min. The cells were washed and incubated with primary antibody (1:100) for 1h at 37^0C. Post washing thrice with phosphate buffer saline (PBS) the cells was incubated with FITC conjugated secondary antibody (1:100) for 1h in dark. The cells were washed and mounting media with 4',6-diamidino-2-phenylindole (DAPI) or propidium iodide (PI) was added to the cells. The slides were analysed using Leics Tcs SP5 laser immunoconfocal microscope.

Preparation of SR9 encapsulated aptamer decorated NPs

Low molecular weight chitosan (2mg/ml) was dissolved in an acetic aqueous solution. Glacial acetic acid was added to bring the pH down (4.5) to dissolve the chitosan. The entrapment method [25] was used for loading of SR9 that was added drop-wise in a known concentration to the chitosan suspension under constant magnetic stirring at 4°C. The LNA EpCAM (LNA Ep) and LNA Nucleolin (LNA Nu) were added to 1mg/ml solution of sodium tri-poly phosphate (STPP) and added drop-wise to the chitosan-SR9 solution. 0.1%(w/v) alginate solution was added to the final mixture and magnetic stirring was done for 24h at 1000 rpm at 4°C. After 24h, the nanoparticle suspension was centrifuged at 2000 rpm for 30 min at 4°C. The pellet obtained was frozen at -80°C overnight and further subjected to lyophilisation (labonco freeze dryer) for a period of 24h. The nanoparticle powder obtained post lyophilisation was stored at 4°C. The EpCAM LNA modified aptamer (LNA-Ep) and nucleolin LNA modified aptamer (LNA-Nu) were dissolved in DNase and RNase free water as the stock solution and stored at -20°C.

Nanoparticle uptake studies

Caco-2, SW480 (colon cancer cells) and FHs-74 Int (healthy gut cells) cells were seeded in 6 well plates and treated with rhodamine labelled chitosan nanoparticles (CHNP-SR9) (10mg/ml) and, 5 and 10 mg/ml of nanobullets for 1h. Nanobullets decorated with scrambled LNA aptamers (5mg/ml) were used as a negative control in this study. Post treatment, cells were washed and lysates were obtained and checked for OD at 530nm. The nanoparticle uptake in mg was calculated using a standard graph plotted using OD of various concentrations of rhodamine labelled CHNP-SR9 and void-CHNP.

Determining the mucoadhesion of nanobullets

The rat intestines were isolated from normal rats, washed with PBS, cut into segments (duodenum, jejunum and ileum). One end was tied by surgical thread and rhodamine-labelled nanobullets were inserted from the other end, the other end was tied as well and the intestine was incubated at 37^0C in RPMI media without phenol red for 4h. After 4 h the loops were cut and the intestine was washed with PBS and fixed with 4% PF overnight. Post fixation intestinal segments were cut into small pieces and stored with optimum cutting temperature (OCT) compound in tissue vials at -80^0C for further use. The frozen tissues were subjected to sectioning in cryotome into a

desired thickness (5-7µm). The tissue sections were placed on glass slides which were fixed with pre cooled acetone (-20^{0}C) for 20 min. Mounting media with DAPI was added to the slide and a cover slip was placed. The slide was viewed using Leics Tcs SP5 laser immunoconfocal microscope.

Tumour spheroid assay with sorted cancer cells

Agarose solution (100µl, 0.1% solution) was added in 96 well plates. Once agar was solidified, cells in a concentration of 1x10³ cells/ml were added, incubated for 7 days at 37°C with 5% CO_2 and formed uniform spheroids in all the wells. In order to determine the difference in internalisation efficacies of non-targeted CHNP-SR9 and nanobullets, the spheroids were incubated with the rhodamine labelled nanoparticles for 1h at 37°C and post treatment the spheroids were fixed with 4% PF for 1h and imaged using Leics Tcs SP5 laser immunoconfocal microscope.

In order to determine the anti-cancer potential the spheroids were treated with 50µg/ml of SR9, 50µg/ml of void CHNP (control CHNP), 50µg/ml of LNA-aptamer targeted NPs and 200nM/ml of 5-fluorouracil (5-FU) for 24h. The tumour spheroids were then analysed using image J software for calculating the spheroid surface area.

In-vivo mouse xenograft studies

Caco-2 cells were used to establish the human colon cancer xenograft model by subcutaneously injecting 2 x 10^5 cells into the left flank of mice. Five-six week old female (*Mus musculus* nude mice-BALB/c nu/nu) were used in the study (n=6). The mice were fed with either AIN93G diet or AIN93G diet which was supplemented with void chitosan NPs and nanobullets (CH-AlNP-SR9-LNA-Nu+Ep). In one group of mice 40mg/kg of 5-FU was injected intra-peritoneally as a drug control. Regular checks were conducted for any sign of physiological or physical distress and mice were weighed thrice a week. At the end of the experimental period the mice were euthanized. Vernier callipers were used to measure the tumour size every week. Biodistribution studies of targeted and non-targeted NCs was conducted by obtaining the fluorescent signals recorded from various parts of the mice including ovary, muscles, bones, eyes, blood, liver, spleen, kidney, lung, heart, brain, stomach, small intestine, large intestine, spinal cord, leg muscles, arm muscles, mesenteric lymph nodes (MLN), tumour site and tissues around the tumour. After 7 days of treatment the tumours were excised and sectioned and stained with annexin V (apoptosis marker), tunnel stain (apoptosis marker) and propidium iodide (PI) (necrosis marker). The respective indices were measured from three tumour sections from the regions of tumour that consisted primarily of healthy proliferating cells mainly found at the margins of the tumour. The necrotic index was measured by counting the cells present in the centre of each tumour. For each tumour specimen 5-10 images were analysed and the average cells positive for annexin V, tunnel and PI were calculated. The cancer stem cells which were only double positive for both CD44 and CD133 (cancer stem cell markers) were taken into account for calculating the number of cells which showed uptake of the NCs.

Statistical analysis

All values were expressed as mean ± S.D. of obtained from at least three experiments unless otherwise stated. For the statistical evaluation of numerical data, one-way ANOVA with Duncan's variance (SPSS 15) was used to compare the groups. P values ≤ 0.05 were considered significant.

RESULTS

Biophysical characterisation of LNA aptamers

The M fold website was used to predict the folded structure of each aptamer (Figure 2A). The LNA modified aptamers used in the present study were analysed using CD spectroscopy for studying their structural configurations and the CD spectra obtained for the LNA-aptamers revealed that both aptamers LNA EpCAM and LNA nucleolin form a G-quadruplex structure (Figure 2B) as their spectra's matched identically with a previously published study [26]. The LNA-EpCAM which is modified version of AS1411 did reveal a change in the CD spectra from the previously published unmodified AS1411 aptamer [27]. The NMR spectra for this EpCAM aptamer has not been reported so far, hence this is the first study to report the NMR spectra of LNA-modified EpCAM aptamer. The 1D 1H NMR spectra of oligonucleotides revealed that the frequency range of the imino proton resonances for LNA EpCAM H-bonded GN1H was between 7.0-7.8 ppm while that of LNA nucleolin was around 6.8 to 7.8. These peaks were not characteristic of G-quadruplex from the previous published report which could be due to the LNA modifications (Figure 2C & D).

Targeting EpCAM and nucleolin

Serum stability studies performed using 10% FBS revealed that LNA nucleolin was more stable than LNA EpCAM as it exhibited high stability until 24h while LNA EpCAM showed slight degradation at 24h (Figure 2E). Confocal studies revealed that both LNA EpCAM and LNA nucleolin were able to bind to their targets with very high specificity within 12 h of treatment. LNA EpCAM (red) could be seen bound to EpCAM (green) present on the cell membrane while LNA nucleolin (red) could be seen bound to nucleolin (green) present in the nucleus (Figure 2F).

Internalisation and anti-cancer efficacy of nanobullets

The SR9 loaded alginate coated chitosan NPs decorated with the LNA aptamers (nanobullets) were observed to be in a size range of 200-300 nm in range whereas the non-alginate coated NPs loaded with SR9 were observed to be in a size range of 50-100 nm (Figure 3A). Table 1 shows effects of different constituents on preparation of NCs. The characterization parameters such as dynamic light scattering spectrometry (DLS), x ray diffraction (XRD), differential scanning colorimetery (DSC) and protein stability were tested using SDS-PAGE and have been previously published [24]. It was observed nearly 0.5-0.8 mg of CHNP-SR9 (10mg/ml) nanoparticles were taken up by Caco-2 and SW480. Less than 0.2 mg of nanobullets 5mg/ml were found to be taken up by all three cell lines. However, nearly 0.4-1.2 mg of 5mg and 10 mg of nanobullets were found to be present in Caco-2 and SW480 cells whereas only 0.2 mg was present in FHs-Int cells suggesting a cancer specific uptake of the nanobullets (Figure 3B). The scrambled LNA aptamer decorated nanobullets showed the least internalisation potential in both normal and cancer cells. The confocal microscopy studies revealed that maximum SR9 (green) was released from the aptamers at 6 h post internalisation (Figure 3C). Confocal microscopy performed for ex-vivo studies using the rat intestine revealed presence of nanobullets on the mucosal surface of the intestinal micro-villi confirming the mucoadhesive nature of these nanobullets (Figure 3D).

Tumour spheroid assay

The tumour spheroid assay revealed that Caco-2 cells were able to form 3D multicellular tumour spheroids in 7 days. Treatment with CHNP-SR9 and nanobullets for 1 h revealed that although CHNP-SR9 showed effective internalisation in the tumour spheroids, yet the nanoparticle intensity in the spheroid core was minimal. On the other hand, the nanobullets showed effectively higher internalisation and incomparable nanoparticle intensity in both spheroid periphery and

the core, suggesting enhanced uptake of nanobullets by the tumour spheroids (Figure 3E). The void CHNP showed a non-significant decrease in the size of the tumour spheroids at 72 h. SR9 on the other hand led to 2.20 fold ($p< 0.05$) reduction in the spheroid size at 24 h and a 3.01 fold ($p\leq 0.01$) reduction in the spheroid size at 72 h. 5-FU on the other hand led to 1.79 fold reduction ($p< 0.05$) at 24 h and 2.85 fold ($p\leq 0.01$) reduction in spheroid size at 72 h. The nanobullets were found to be the most effective as they led to a 2.26 fold ($p< 0.05$) reduction at 24 h and a 4.95 fold reduction ($p\leq 0.001$) fold reduction in the spheroid size at 72 h (Figure 3F).

Efficacy of nanobullets in a colon cancer mouse xenograft model

The body weight analysis from mice revealed no significant increase or decrease in the mice weight in control (untreated) and nanobullets fed mice. The void CHNP fed mice also showed a similar pattern in the body weight with no-significant decrease (Figure 4A). In order to determine the targeting potential of the synthesized nanobullets, *in-vivo* biodistribution studies were carried out. There was no significant difference observed between the uptake of control CHNP and nanobullets in the tumour. However, the control CHNP were found to be significantly more in liver, kidney, lung, brain, bone, mesenteric lymph nodes (MLN) and also around the tumour when compared to the nanobullets that were also observed to be higher in the blood and small intestine (Figure 4B). The anti-cancer potential of nanobullets was determined by studying their effect on the tumour volume. We observed that the tumour regression was apparent (4 fold higher) in mice treated with nanobullets for nearly 70 days. Although 5-FU showed an initial lowering in tumour size, however failed to induce any further substantial reduction in tumour. The mice fed with the void NCs (control CHNP) supplemented diet showed increased tumour volume with time (Figure 4C). The nanobullets showed substantial *in-vivo* internalization (8 fold higher, $p\leq 0.01$) in EpCAM, CD44 and CD133 positive cancer stem cells when compared to the void NPs. The nanobullets were able to show a significantly high apoptotic (10 fold, $p\leq 0.01$) and necrotic index in the tumour cells (12.5, p $p\leq 0.01$) when compared to void NPs. The apoptotic index obtained by both annexin V and tunnel staining showed significant effects the treatments ($p\leq 0.001$ and $p\leq 0.01$) (Fig 4D).

DISCUSSION

Our findings from this study have shown that in cancer cells EpCAM is majorly expressed on the cell membrane, whereas in normal cells the majority of EpCAM expression is within the cytoplasm or inside the nucleus (Figure S1). Previously published studies have shown that EpCAM in normal cells is predominantly located inside the cells and holds the capability to translocate inside the nucleus[28]. Nucleolin LNA aptamers was used in this study because it has been reported that nucleolin also exists at low levels on the cell surface of Caco-2 cells [29] however, in cancer stem cells majority of nucleolin is known to be expressed in nucleus (translocates from surface to nucleus) and inhibits p53 pathway to maintain the embryonic stem cell self-renewal capability [30]. Hence, targeting nucleolin using LNA may ensure enhanced uptake of nanobullets/LNP's ensuring the cancer-specific delivery of nanoformulated SR9. It has also been proved earlier that LNA-aptamer conjugated NPs are highly effective in cancer-specific targeting and induce cancer-specific cytotoxicity while being harmless to non-cancerous cells [31, 32].

The aptamers used to target EpCAM is an RNA oligonucleotide previously published as EpdT3 [33] to target EpCAM in retinoblastoma cells. However, in the present study we incorporated three LNA modifications in the same sequence in order to enhance the stability of these aptamers. This is the first study therefore to

determine the stability, structure and characterization of this aptamer. On the other hand, the well-established AS1411 aptamer [27] has been used to target nucleolin. However, this is the first study where LNA modifications have been incorporated in AS1411 and we have reported the stability, structure and characterization of this LNA modified aptamer as well. The guanosine residues were chosen in the present study since G-C bond is stronger than A-T bonds, moreover both sequences were rich in guanosine residues. The LNA modification were majorly made in the stem region so as not to harm the binding ability of the aptamers.

Guanine (G)-quadruplexes are highly stable nucleic acid secondary structures formed from association of short G-rich sequences. These can occur in both DNA and RNA. CD and NMR spectroscopy are two methods commonly used to characterise presence of G-quadruplexes in oligonucleotides. Increase in peak intensity at 260 nm and frequency range of the imino protons between 10-12 ppm is considered characteristic for presence of G-quadruplexes using CD and NMR spectroscopy respectively [27]. In the present study, the CD spectra of a LNA EpCAM and LNA nucleolin increase in peak intensities were observed at 260nm. Our results were compared to those of a previously published study[34] confirming presence of G-quadruplexes in both the LNA aptamers. However, there were some changes observed in the NMR spectra of the LNA modified aptamers from the standard G-quadruplex spectra. Studies have reported that a modification at either the 3' or 5' end may lead to absence or shift in the G-quadruplex peaks [35]. The LNA modifications were made at both 3' and 5' end which may be the reason for shift in the peaks characteristic of G-quadruplexes. The targeting studies (confocal microscopy) revealed that these modifications did not alter the functioning and targeting ability of these aptamers and since the LNA modifications are known to increase the stability of the aptamer as shown in the present study, it can be inferred that the modifications made were successful.

Chitosan and alginate are proved to be bio-compatible and used in medical applications. Even though, there is evidence regarding mild toxicity of chitosan derivatives and solution form of chitosan and its salts at low pH [36], careful handling of chitosan promises several health benefits [37]. Alginate has been approved by the US Food and Drug Administration (FDA) for its oral use [38]. Hence both these natural, biodegradable and biocompatible polymers were used in the present study for nanobullet synthesis. Determination of cell proliferation using Cy-Quant assay revealed the non-cytotoxic nature of these polymers (Figure S2). In the present study, mice treated with diet carrying nanocarriers showed no abnormality with respect to body weight and behavioural changes. Thus, any questions of nano-toxicity could be nullified.

The mechanism of interaction of chitosan with human cells has been studied in several laboratories and it is proposed that chitosan enters the target cells by a combination of bioadhesion (due to being mucoadhesive) and a transient widening of tight junctions between the ocular cells [39]. It has been previously reported that chitosan increases transcellular permeability in human and rat intestinal mucosa [40]. Chitosan also induced a non-inflammatory microenvironment within the intestinal epithelium and generated formation of large vacuoles. It triggered release of arachidonic acid in intestinal epithelial cells which aided in mucoadhesiveness of the polymer [41]. In the present study, adhesion of nanobullets on the rat intestinal mico-villi surface confirms the mucoadhesive nature of these nanobullets. The in vitro nanoparticle uptake studies revealed that 10 mg/ml of nanobullets showed a 1.73 fold higher uptake in SW480 and a 1.6 fold higher uptake in Caco-2 cells when compared to CHNP-SR9. Previous studies have revealed that SW480 showed higher expression of mucin-1 (Muc-1) than Caco-2 [24], which could

be the reason for higher uptake in SW480 cells. In our previous studies we have shown that blocking Muc-1 receptors leads to a decrease in uptake of CHNP-SR9 [24]. The reason for this is that, chitosan gets adsorbed to mucosal surface (containing mucin) by showing electrostatic interaction with sialic acid (present in Muc receptors) and the intensity of its adsorption is directly proportional to sialic acid content [42]. A minimal uptake in the healthy intestinal cells (FHs 74 Int), confirm a successful cancer specific uptake of the LNA aptamer decorated nanobullets.

Tumour spheroids models are generally established to eliminate the ineffective drugs at pre-animal and pre-clinical state and also in order to identify the promising drugs. The spheroid model forms an intermediate environment relative to monolayer and *in-vivo* models [43]. The necrotic core in the multicellular tumour spheroids is commonly related to nutrient deprivation, and is believed to contain the cancer stem cells and the drug resistant cells [44]. It is believed that most drugs mainly target proliferating cells, while the dormant cancer cells acquire resistance to such anti-cancer drugs. Therefore, treatments that have the ability to target cancer cells in poorly vascularized tumor regions may have the potential to enhance cytostatic-based chemotherapy of solid tumors [45]. In the present study, we found that the nanobullets had the ability to target both the periphery and the core of the multicellular tumour spheroids. This ability was imparted to these nanoparticles mainly by the LNA aptamers as the non-targeted CHNP-SR9 failed to internalise in the spheroid core within the same treatment period.

We also showed efficacy of SR9 to reduce the 3D tumour spheroid size in comparison with 5-FU. The nanobullets on the other were reasonably better in reducing the size of the tumour spheroids than both SR9 and 5-FU. This is primarily due to the fact that they were able to internalize effectively and reach the core of the tumour spheroids. The *in-vivo* nanoparticle biodistribution studies showed that both the targeted as well as the void NCs showed nearly 7 fold higher internalization in tumour site when compared to other body parts of the mice. This could mainly be due to the enhanced permeability retention (EPR) effect and also due to tumour specific targeting of the targeted NCs. The void NCs showed more accumulation in other parts of the mice such as muscle, bone, eye, liver, spleen, kidney, lungs, brain, spinal cord, MLN and around the tumour site. The aptamer decorated nanobullets showed 4 fold reduction in the tumour volume at the end of the study (70^{th} day) when compared to the void NCs and the apoptotic vs necrosis index showed nearly 13.3 fold higher annexin V, 9.2 Tunnel and 7 fold high PI staining when compared to void NCs treated mice. SR9 has the ability to bind to the wild type survivin in order to form a heterodimer [24, 46, 47]. This affinity of SR9 towards the wild type survivin is the reason for cancer specific cytotoxicity. The number of cancer stem cells that showed uptake of nanobullets was also 6 fold higher when compared to void nanocarrier treated mice.

TABLE

FIGURE AND FIGURE LEGENDS

Figure 1. Locked nucleic acid modified aptamer decorated nanoparticles: Locked nucleic acid-nanoparticle conjugate (LNP) was prepared using LNA EpCAM, LNA nucleolin, chitosan, alginate and STPP (termed nanobullets), encapsulating a cell permeable dominant-negative survivin protein (SR9) that can target EpCAM and nucleolin expression to induce cancer and cancer stem cell-specific apoptosis.

Figure 2. Targeting EpCAM and nucleolin using LNA aptamers: A) The M fold structures of the LNA nucleolin (DNA) aptamer and the LNA EpCAM (RNA) aptamer. B) The circular dichroism (CD) spectra of LNA EpCAM and LNA nucleolin revealed presence of G-quadruplex conformation of the aptamers. C) 1D ^{1}H NMR spectrum of LNA nucleolin and D) LNA EpCAM in 10% D_2O/H_2O obtained at 500MHz. E) The serum stability tests revealed that both LNA-Nucleolin and LNA-EpCAM were highly stable in 10% serum until 24h. F) Confocal microscopy confirmed that both EpCAM and nucleolin LNA aptamers (red) were able to bind to their targets (green) with very high specificity within 12 h of treatment.

Figure 3. Internalisation and anti-tumour efficacy of nanobullets: A) The SEM images show spherical shape and size of CHNP-SR9 (50-100 nm) and CHAlNP-SR9 (200-300nm). B) The LNA aptamer decorated nanobullets demonstrated an enhanced cancer-specific uptake. C) Confocal microscopy revealed release of maximum SR9 (green) at 6 h post internalisation in Caco-2 cells (red). D) The ex-vivo studies revealed the presence of rhodamine labelled nanobullets (red) on the mucosal surface of the rat intestinal micro-villi (blue). E) The rhodamine labelled nanobullets (red) showed effectively higher internalisation in both periphery and the core of spheroids compared to CHNP-SR9. F) The nanobullets were most effective as they led to a 2.26 fold ($p< 0.05$) reduction at 24 h and a 4.95 fold reduction ($p\leq 0.001$) fold reduction in the spheroid size at 72 h. The tumour regression was 4 fold higher in mice fed on nanobullet diet when compared to control diet.

Figure 4. *In-vivo* studies with double aptamer decorated nanobullets showed regression in tumours when fed orally: A) Body weight analysis from mice showed no significant change in the untreated and the nanobullets fed mice. B) The nanocarrier biodistribution studies showed that the NCs were highly specific to the tumour since their maximum uptake was in the tumour cells when compared to other organs and tissues of the mice. C) The targeted LNP's were successfully able to suppress the tumour growth up to 70 days which was highly significant when compared to the control diet. D) The apoptotic index, the necrotic index and the number of nanocarrier uptake was much higher in case of targeted NCs when compared with void (control) NPs.

CONCLUSION

The nanobullets target cancer cells and cancer stem cells mainly due to expression of markers such as EpCAM, nucleolin, and survivin. The nanobullets are translocated into cytoplasm of cancer cells due to the high apical expression of EpCAM and they are translocated into the nucleus due to high surface expression of nucleolin. Mucoadhesion also helps nanobullets to internalize by paracellular pathways and the nanobullets are highly capable of internalizing by endocytosis. Using dominant negative survivin ensured cancer-specific cytotoxicity. Hence, our studies have shown a highly specific cancer cell and cancer stem cell targeted therapeutic approach.

ACKNOWLEDGEMENTS

The authors would like to thank the Australia–India Strategic Research Fund (AISRF BF030016), National Health and Medical Research Council (NHMRC APP1050286) and Australian Research Council for funding Deakin University's Magnetic Resonance Facility through LIEF grant (LE110100141) for financial support. The authors would also like to thank Ms *Gail Dyson* from *Deakin University* (Faculty of Science Engineering & Built Environment) for her guidance with the NMR. The authors have no other relevant

affiliations or financial involvement with any organization or entity with a financial interest in or financial conflict with the subject matter or materials discussed in the manuscript apart from those disclosed. No writing assistance was utilized in the production of this manuscript.

Notes and references

[1] Nanomedicine-Laboratory of Immunology and Molecular Biology (NLIMBR), Faculty of Health, School of Medicine, Deakin University, 75 Pigdons Road, Waurn Ponds, Geelong, Victoria 3217, Australia.

[2] Department of Pharmacology, College of Medicine, National Cheng Kung University, Tainan, Taiwan R.O.C.

[3] Institute of Basic Medical Sciences, College of Medicine, National Cheng Kung University, Tainan, Taiwan R.O.C.

[4] Research Centre for Chemistry and Biotechnology, School of Life and Environmental Sciences, Deakin University, Waurn Ponds, Victoria, 3216, Australia.

[5]Nucleic Acid Center, Department of Physics, Chemistry and Pharmacy, University of Southern Denmark, Campusvej 55 Odense M 5230 Denmark; School of Chemistry and Molecular Biosciences, University of Queensland, St Lucia, Brisbane, 4072 Australia.

[6] Larsen and Toubro Department of Ocular Pathology, Vision Research Foundation, Sankara Nethralaya, Chennai, India.

Corresponding Author

Jagat R. Kanwar * Tel: 0061 3 52271148; Fax: 0061 3 52272539;

Email: jagat.kanwar@deakin.edu.au

Jagat R. Kanwar, Nanomedicine-Laboratory of Immunology and Molecular Biology (NLIMBR), Faculty of Health, School of Medicine, Deakin University, 75 Pigdons Road, Waurn Ponds, Geelong, Victoria 3217, Australia.

REFERENCES

1. F. A. Haggar and R. P. Boushey, *Clin Colon Rectal Surg*, 2009, **22**, 191-197.
2. Jemal A, Bray F, Center MM, Ferlay J and Forman D, *CA Cancer J Clin*, 2011, **61**, 69-90.
3. Watson AJM, *Gut* 2004, **53**, 1701-1709.
4. O. T. Zhang T, Gao Z, Gao Z, Ehrlich SM, Fields JZ, Boman BM,, *Cancer Res*, 2001 **61**, 8664-8667.
5. C. H. Cheung, X. Sun, J. R. Kanwar, J. Z. Bai, L. Cheng and G. W. Krissansen, *Cancer Cell Int*, 2010, **10**, 36.
6. M. Munz, P. A. Baeuerle and O. Gires, *Cancer Research*, 2009, **69**, 5627-5629.
7. O. Gires, C. A. Klein and P. A. Baeuerle, *Nat Rev Cancer*, 2009, **9**, 143-143.
8. P. Dalerba, S. J. Dylla, I. K. Park, R. Liu, X. H. Wang, R. W. Cho, T. Hoey, A. Gurney, E. H. Huang, D. M. Simeone, A. A. Shelton, G. Parmiani, C. Castelli and M. F. Clarke, *P Natl Acad Sci USA*, 2007, **104**, 10158-10163.
9. P. H. Srivastava M, *FASEB J*, 1999, **13**, 1911-1922.
10. Derenzini M, *Micron*, 2000, **31**, 117–120.
11. O. R. Semenkovich CF, Olson MO, Yang JW,, *Biochemistry*, 1990, **29**, 9708–9713.
12. A. G. Hovanessian, F. Puvion-Dutilleul, S. Nisole, J. Svab, E. Perret, J. S. Deng and B. Krust, *Exp Cell Res*, 2000, **261**, 312-328.
13. C. M. Chen, S. Y. Chiang and N. H. Yeh, *Journal of Biological Chemistry*, 1991, **266**, 7754-7758.
14. Y. Otake, S. Soundararajan, T. K. Sengupta, E. A. Kio, J. C. Smith, M. Pineda-Roman, R. K. Stuart, E. K. Spicer and D. J. Fernandes, *Blood*, 2007, **109**, 3069-3075.
15. M. Pavsic, G. Guncar, K. Djinovic-Carugo and B. Lenarcic, *Nature communications*, 2014, **5**, 4764.
16. S. Arumugam, M. C. Miller, J. Maliekal, P. J. Bates, J. O. Trent and A. N. Lane, *Journal of biomolecular NMR*, 2010, **47**, 79-83.
17. S. Imrich, M. Hachmeister and O. Gires, *Cell Adh Migr*, 2012, **6**, 30-38.
18. G. Spizzo, D. Fong, M. Wurm, C. Ensinger, P. Obrist, C. Hofer, G. Mazzoleni, G. Gastl and P. Went, *J Clin Pathol*, 2011, **64**, 415-420.
19. S. Denzel, D. Maetzel, B. Mack, C. Eggert, G. Barr and O. Gires, *BMC Cancer*, 2009, **9**, 402.
20. Zhou G, Seibenhener ML and Wooten MW, *Journal of Biological Chemistry* 1997, **272**, 31130-31137.
21. J. R. Kanwar, R. R. Mohan, R. K. Kanwar, K. Roy and R. Bawa, *Nanomedicine (Lond)*, 2010, **5**, 1435-1445.
22. W. J. Veedu RN, *RNA Biol*, 2010, **6**, 321-323.
23. R. N. Veedu and J. Wengel, *Chem Biodivers*, 2010, **7**, 536-542.
24. K. Roy, R. K. Kanwar, S. Krishnakumar, C. H. A. Cheung and J. R. Kanwar, *International journal of nanomedicine*, 2015, **10**, 1019.
25. MacLaughlin FC, Mumper RJ, Wang J, Tagliaferri JM, Gill I, Hinchcliffe M and Rolland AP, *J Control Release*, 1998, **56**, 259-272.
26. A. R. Haeusler, C. J. Donnelly, G. Periz, E. A. Simko, P. G. Shaw, M.-S. Kim, N. J. Maragakis, J. C. Troncoso, A. Pandey and R. Sattler, *Nature*, 2014, **507**, 195-200.
27. M. M. Dailey, M. C. Miller, P. J. Bates, A. N. Lane and J. O. Trent, *Nucleic acids research*, 2010, **38**, 4877-4888.
28. Munz M, Baeuerle PA and Gires O, *Cancer Res*, 2009, **69**, 5627-5629.
29. K. Dean P, *Microbiology*, 2011, **157**, 1761-1767.
30. S. G. Yang A, Zhou C, Lu R, Li H, Sun L, Jin Y,, *J Biol Chem*, 2011, **286**, 43370-43382.
31. J. R. Kanwar, R. K. Kanwar, G. Mahidhara and C. H. A. Cheung, *Aust J Chem*, 2012, **65**, 5-14.
32. J. R. Kanwar, K. Roy and R. K. Kanwar, *Crit Rev Biochem Mol Biol*, 2011, **46**, 459-477.
33. Adida C, Gaulard P, Lepage E, Morel P, Briere J, Dombret H, Reyes F, Diebold J, Gisselbrecht C, Salles G, Altieri DC and Molina TJ, *Blood*, 2000, **96**, 1921-1925.
34. P. Fratta, S. Mizielinska, A. J. Nicoll, M. Zloh, E. M. Fisher, G. Parkinson and A. M. Isaacs, *Scientific reports*, 2012, **2**.

35. Markowska M, Oberle R, Juzwin S, Hsu CP, Gryszkiewicz M and Streeter AJ, *J Pharmacol Toxicol Methods*, 2001, **46**, 51-55.
36. P. Baldrick, *Regul Toxicol Pharmacol*, 2010, **56**, 290-299.
37. M. D. Gades and J. S. Stern, *J Am Diet Assoc*, 2005, **105**, 72-77.
38. F. Tugcu-Demiroz, F. Acarturk, S. Takka and O. Konus-Boyunaga, *Eur J Pharm Biopharm*, 2007, **67**, 491-497.
39. P. Artursson, Lindmark, T., Davis, S.S., Illum, L., *Pharm. Res.*, 1994, **11**, 1358-1361.
40. L. P. P. M. Magdalena Canalia, Jesús Balsindeb, Cristina Ibarrac, Silvia G. Correa, *European Journal of Pharmaceutics and Biopharmaceutics*, 2012, **80**, 418–425.
41. Deacon MP, McGurk S, Roberts CJ, Williams PM, Tendler SJ, Davies MC, Davis SS and Harding SE, *Biochem. J*, 2010, **348**, 557–563.
42. P. He, S. S. Davis and L. Illum, *International Journal of Pharmaceutics*, 1998, **166**, 75-88.
43. Hirschhaeusera F, Menneb H, Dittfeldc C, Westb J, Mueller-Kliesera W and Kunz-Schughart LA, *Journal of Biotechnology*, 2010, **148**, 3-15.
44. A. Bertuzzi, A. Fasano, A. Gandolfi and C. Sinisgalli, *Journal of theoretical biology*, 2010, **262**, 142-150.
45. C. Wenzel, B. Riefke, S. Gründemann, A. Krebs, S. Christian, F. Prinz, M. Osterland, S. Golfier, S. Räse and N. Ansari, *Experimental cell research*, 2014, **323**, 131-143.
46. T. R. McKay, S. Bell, T. Tenev, V. Stoll, R. Lopes, N. R. Lemoine and I. A. McNeish, *Oncogene*, 2003, **22**, 3539-3547.
47. J. R. Kanwar, W. P. Shen, R. K. Kanwar, R. W. Berg and G. W. Krissansen, *J Natl Cancer I*, 2001, **93**, 1541-1552.

A table of contents entry:

EpCAM and nucleolin translocate into the cytoplasm and nucleus that facilitates enhanced uptake of nanocarrier to specifically target cancer cells.

Table 1. Effect of different constituents in preparation of NCs.

Sample Number	Constituents (Ratio)	Conditions	Size and shape	Loading capacity (%)	Association efficiency (5)
1	Chitosan:STPP (2:1)	1000 rpm, 24 h at 4 ℃	300 nm± 20 nm (spherical)	-	-
2	Chitosan:STPP:Alginate (2:1:1)	1000 rpm, 24 h at 4 ℃	1000 nm± 20 nm (spherical)	-	-
3	Chitosan:SR9:STPP (2:0.25:1)	1000 rpm, 24 h at 4 ℃	60 nm± 10 nm (spherical)	15.36%	92.19%
4	LNA-EpCAM+LNA-Nucleolin-Chitosan:SR9:STPP:Alginate (2:0.25:1:1)	1000 rpm, 24 h at 4 ℃	75 nm± 20 nm (spherical)	18.2%	86.24%

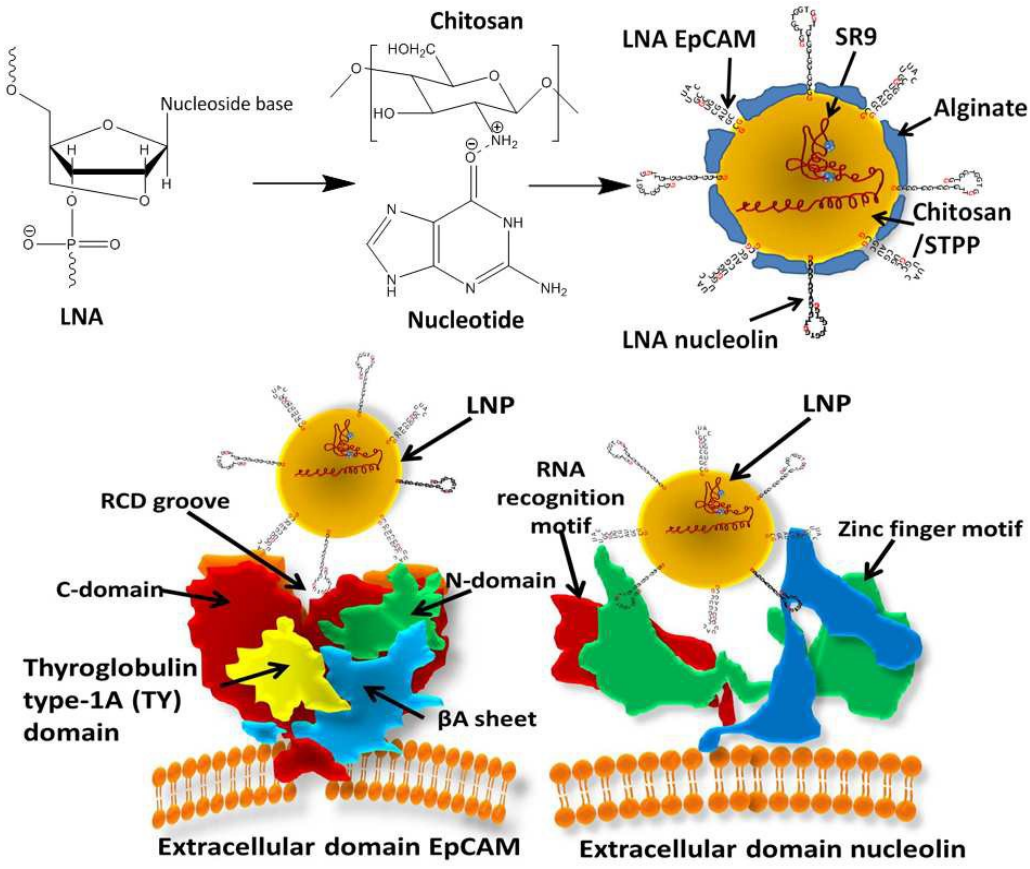

Figure 1. Locked nucleic acid modified aptamer decorated nanoparticles: Locked nucleic acid-nanoparticle conjugate (LNP) was prepared using LNA EpCAM, LNA nucleolin, chitosan, alginate and STPP (termed nanobullets), encapsulating a cell permeable dominant-negative survivin protein (SR9) that can target EpCAM and nucleolin expression to induce cancer and cancer stem cell-specific apoptosis.

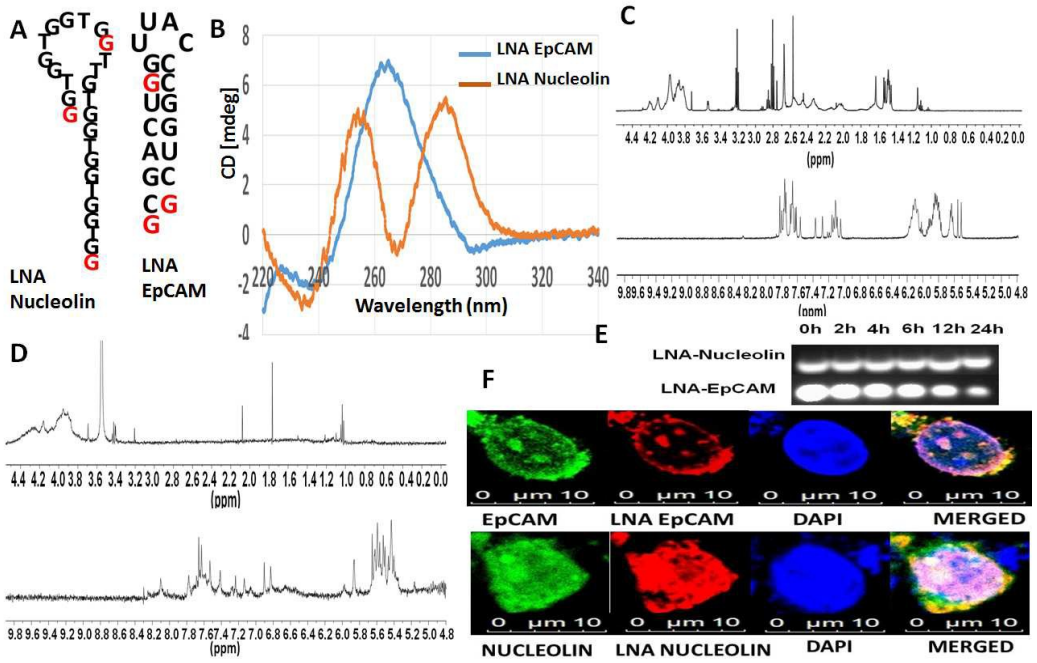

Figure 2. Targeting EpCAM and nucleolin using LNA aptamers: A) The M fold structures of the LNA nucleolin (DNA) aptamer and the LNA EpCAM (RNA) aptamer. B) The circular dichroism (CD) spectra of LNA EpCAM and LNA nucleolin revealed presence of G-quadruplex conformation of the aptamers. C) 1D 1H NMR spectrum of LNA nucleolin and D) LNA EpCAM in 10% D2O/H2O obtained at 500MHz. E) The serum stability tests revealed that both LNA-Nucleolin and LNA-EpCAM were highly stable in 10% serum until 24h. F) Confocal microscopy confirmed that both EpCAM and nucleolin LNA aptamers (red) were able to bind to their targets (green) with very high specificity within 12 h of treatment.

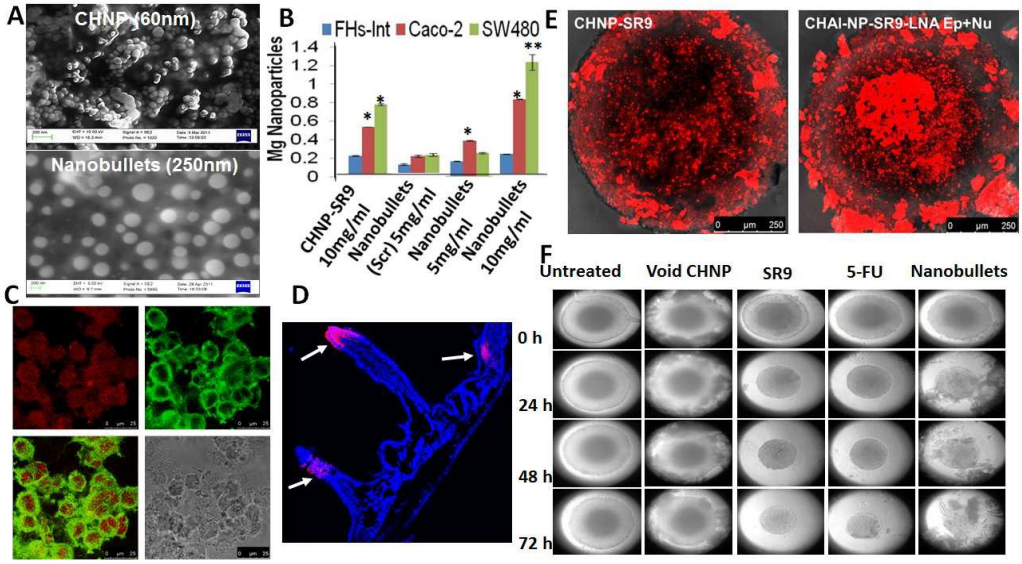

Figure 3. Internalisation and anti-tumour efficacy of nanobullets: A) The SEM images show spherical shape and size of CHNP-SR9 (50-100 nm) and CHAlNP-SR9 (200-300nm). B) The LNA aptamer decorated nanobullets demonstrated an enhanced cancer-specific uptake. C) Confocal microscopy revealed release of maximum SR9 (green) at 6 h post internalisation in Caco-2 cells (red). D) The ex-vivo studies revealed the presence of rhodamine labelled nanobullets (red) on the mucosal surface of the rat intestinal micro-villi (blue). E) The rhodamine labelled nanobullets (red) showed effectively higher internalisation in both periphery and the core of spheroids compared to CHNP-SR9. F) The nanobullets were most effective as they led to a 2.26 fold ($p < 0.05$) reduction at 24 h and a 4.95 fold reduction ($p \leq 0.001$) fold reduction in the spheroid size at 72 h. The tumour regression was 4 fold higher in mice fed on nanobullet diet when compared to control diet.

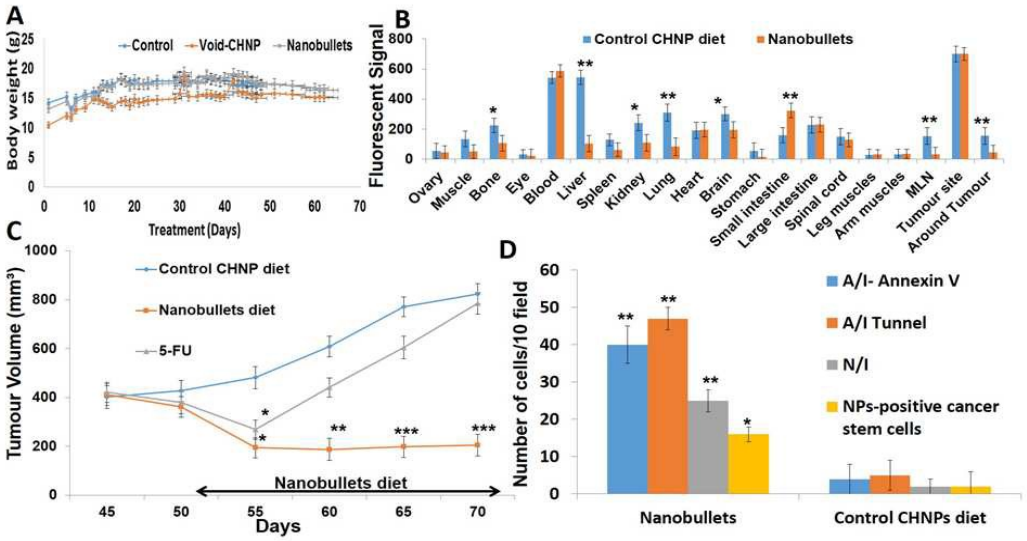

Figure 4. In-vivo studies with double aptamer decorated nanobullets showed regression in tumours when fed orally: A) Body weight analysis from mice showed no significant change in the untreated and the nanobullets fed mice. B) The nanocarrier biodistribution studies showed that the NCs were highly specific to the tumour since their maximum uptake was in the tumour cells when compared to other organs and tissues of the mice. C) The targeted LNP's were successfully able to suppress the tumour growth up to 70 days which was highly significant when compared to the control diet. D) The apoptotic index, the necrotic index and the number of nanocarrier uptake was much higher in case of targeted NCs when compared with void (control) NPs.